Ultrasonic Evaluation of Bone Callus Growth in a Rabbit Tibial Distraction Model

H.K. Luk , Y.M. Lai , L. Qin , C.W. Chan , Z. Liu , Y.P. Huang , Y.P. Zheng

Abstract—Ultrasound is useful in demonstrating bone mineral density of regenerating osseous tissue as well as structural alterations. A proposed ultrasound method, which included ultrasonography and acoustic parameters measurement, was employed to evaluate its efficacy in monitoring the bone callus changes in a rabbit tibial distraction osteogenesis (DO) model.

The findings demonstrated that ultrasonographic images depicted characteristic changes of the bone callus, typical of histology findings, during the distraction phase. Follow-up acoustic parameters measurement of the bone callus, including speed of sound, reflection and attenuation, showed significant linear changes over time during the distraction phase. The acoustic parameters obtained during the distraction phase also showed moderate to strong correlation with consolidated bone callus density and micro-architecture measured by micro-computed tomography at the end of the consolidation phase.

The results support the preferred use of ultrasound imaging in the early monitoring of bone callus changes during DO treatment.

Keywords—Bone Callus Growth, Rabbit Tibial Distraction Osteogenesis, Ultrasonography, Ultrasonometry

I. INTRODUCTION

DISTRACTION osteogenesis (DO) is an advanced biological treatment for bone regeneration in patients suffering from pathologies such as dwarfism and other limb deformities. The most critical stages in the DO treatment are during the distraction and consolidation phases. Under the external tensile loading during distraction, the physical structure and the cellular responses of the bone callus spatially and temporally undergo changes [1, 2]. These growth changes are highly related to the final outcome of DO treatment [1, 3]. Thus, close and constant monitoring of the healing status, especially at the early DO stage, is very important for customizing healing factors such as distraction rate and rhythm [1, 2].

Conventional radiography is commonly used to monitor bone callus density changes during DO treatment. However, because of the non-linear characteristic of the film-screen combination, it limits the detection of the initial bone formation, which has subtle density changes during the early DO stage [3].

Quantitative computed tomography (qCT) allows the three-dimensional (3D) evaluation of bone tissues and measures their physical and morphological properties[2]. However, the image artifact, which results from the external

1. Department of Health Technology and Informatics, The Hong Kong Polytechnic University, Hong Kong, P.R.China.
2. Department of Orthopaedics and Traumatology, The Chinese University of Hong Kong, Hong Kong, P.R.China.
3. School of Chinese Medicine, The Chinese University of Hong Kong, Hong Kong, P.R.China.
*   Corresponding Author: Tel.: (852) 3400 8565; Fax: (852) 2362 4365. E-mail address: htymlai@inet.polyu.edu.hk (Dr. Yau Ming LAI).

metallic distractor, causes inaccuracy in the bone properties measurement [1, 3] and the high radiation dose, which occurs in follow-up CT measurements, may deter its application in paediatric DO patients [4].

Ultrasonography (US), a non-ionizing and non-invasive imaging modality, allows repeatable clinical measurements [5] and previous studies reported that US had the ability to detect early new bone formation during fracture healing [6, 7]; however, the subjective ultrasonographic interpretation of the bone callus growth may prevent a valid comparison with its quantitative callus measurement [1]. Ultrasonometric parameters, such as acoustic reflection, attenuation and backscattering, have been widely investigated in *in-vitro* studies, which showed high correlation with the physical characteristics of bone tissues [8, 9]. However, there have been few studies using both ultrasonographic images and ultrasonometric parameters to evaluate the *in-vivo* bone callus growth.

In light of the above review, we proposed a US method which included *in-vivo* ultrasonography and acoustic parameters measurement for monitoring the growth condition of bone callus in a rabbit tibial DO model. The predictive power of these acoustic parameters obtained during DO treatment was evaluated with the end-point evaluation of the bone callus properties using micro-computer tomography (μCT).

II. MATERIALS AND METHODS

A. Animal and Surgical Intervention

The distraction model was established in several previous studies [10-13]. Animal surgical procedures were performed with the permission of the local government animal protection authorities and the university ethical committee. Seven male New Zealand white rabbits (28th-34th week and 3.0-4.0 kg) were anesthetized with an intramuscular injection consisting of ketamine (75mg/kg) and xylazine (10mg/kg). The surgical incision was performed at the antero-medial mid-diaphyseal region of the right tibia, where the periosteum and tibial muscles were elevated and preserved. The medial tibial surface was exposed for drilling and sawing. To ensure the drilling direction was perpendicular to the bone longitudinal axis, the bicortical predrilling of four pin holes was conducted with researcher-designed acrylic drill-guides. Pin holes were produced by an air drill (Synthes International, German) with a 1.5 mm drill bit and then a 2.0 mm bit. The unilateral external distractor was used as a template for inserting four 2.0-2.5 mm

self-taping pins (Orthofix International, Italy) into pin holes (Fig. 1). A low-energy oscillating osteotomy was performed between the 2nd and 3rd pins at a position just below the tibiofibular junction. During the sawing, the periosteum and soft tissues were protected by the periosteal elevator. After sawing, a proper bone alignment was ensured before loading the distractor. Before the closure of the surgical wound, the periosteum and tibial muscles were returned to their original position. Analgesic drug, Temgesic® (0.3mg/kg) was administered to the rabbits for three consecutive days following osteotomic surgery and their health and behaviour were monitored daily.

Fig. 1 Photograph demonstrates the pin insertion into the predrilled tibial bone during DO surgery

B. Distraction Protocol

The tibial distraction began eight days after osteotomy. All rabbits were distracted under a constant distraction rate of 1.0 mm/day, a two-step 0.5-mm increment with a six-hour separation. This rate and rhythm were considered standard clinical practice in the human DO treatment [14, 15] and were also previously applied in the rabbit tibial model [10]. Temgesic® (0.12mg/kg) was administered to the animals 30 minutes prior to conducting each distraction.

A tibial length of 12 mm was distracted over 12 consecutive days. After the distraction period, the consolidation period was initiated on day 20 until day 47, a period of nearly four weeks. The external distractor was left *in-situ* during consolidation.

C. Imaging Evaluation

Since the bone callus had differential growth changes in its regions [16, 17], three equal callus regions at the distal, middle and proximal positions were used for spatial and temporal comparison of US and µCT measurements during imaging evaluation.

In addition to the use of post-operative radiography to assess the bone alignment, the bone callus growth in its three regions was studied by US at the end of latency. This was followed by a 3-day and weekly interval of the same imaging evaluation during 12-day distraction and 4-week consolidation periods, respectively.

After the *in-vivo* measurement, all rabbits were euthanized at the end of the consolidation phase (day 47), by an intravenous overdose injection of 20% pentobarbital. External distractors

were *in situ* and tibial samples were kept in -20°C before µCT scanning.

1. US Study

i. Ultrasound System Configuration

A broadband linear ultrasound probe (Terason Corporation, USA) with a dimension in 35.0 mm (L) x 10.0 mm (W) was connected to an ultrasound system (Terason Corporation, USA) for collecting the radio-frequency (RF) signals reflected from bone callus. According to the measurement of the acoustic reflection from a planar steel plate immersed in a water tank, the central frequency of the transducer was 6 MHz with an effective bandwidth from 4-8 MHz.

ii. US Longitudinal Measurement (US L-scan)

The transducer was manually placed parallel to the distractor and above the bone callus (Fig. 2). Before applying sterile ultrasound gel (Parker Lab Inc., USA) to the skin-transducer interface, hair on the distracted leg was shaved to enhance the surface coupling. In each US imaging, a B-mode image and its RF signals were automatically recorded in JPEG and ULT format, respectively.
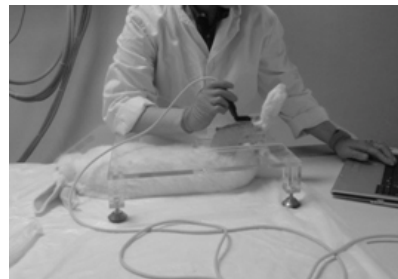

Fig. 2 Photograph demonstrates the longitudinal ultrasonographic measurement at the distracted tibia of anesthetized rabbit

JPEG images were compared temporally at different time points along DO treatment. ULT data were rebuilt and graphically shown in a MatLab researcher-designed graphic user interface (MathWorks Inc., USA). In each reconstructed image, a rectangular ROI was manually contoured on the bone callus for measuring the acoustic parameters. The depth of the ROI was consistently 6.0 mm while its breadth depended on the distracted tibial length at the measurement time point.

For acoustic parameters calculation, the reference speed of sound (SoS_0) measured by a planar steel plate immersed in a water tank was 1.54 mm/µs. Also, reference signals for different depths were collected from the acoustic reflection of the steel plate. Before the parameters calculation, RF signals in the ROI were all corrected with the system gain and used for calculating the integrated reflection (IRC), integrated attenuation (IA) and corrected integrated backscattering (IBS_{corr}) of the bone callus.

iii. Estimation of Callus Speed of Sound (SoS_cal)

There was prior knowledge that the density and speed of sound in the callus (SoS_{cal}, mm/μs) would be increased by the bone mineralization during DO treatment [8, 14, 17] and also that the change of SoS_{cal} would influence the effective depth of ROI used for the acoustic parameters calculation. Thus, SoS_{cal} had to be estimated to adjust the effective depth of ROI.

Literatures addressing the issue of bone callus density changes at different stages throughout DO treatment were found to be sparse. Instead, a researcher-defined equation was established, which assumed that SoS_{cal} exponentially increased throughout DO treatment and correlated with the reflection coefficient of the callus (R_{cal}), the ratio between the maximum amplitudes of the acoustic reflections obtained from callus at the measurement time point and the planar steel plate. The equation was defined as:

$$SoS_{cal} = SoS_{cor} * e^{\frac{(R_{cal} - R_{cor})}{R_{cor}}} \qquad (1)$$

where SoS_{cor} was the speed of sound of the cortical bone measured in the transverse direction and assumed to be 3.44 mm/μs [18]; and R_{cor} was the reflection coefficient of the cortical bone, the ratio between the maximum amplitudes of the acoustic reflection obtained from the tibial cortical segments on day 7 (i.e. before the distraction) and the planar steel plate.

The development of this equation was based on the exponential increment of the callus acoustic impedance during DO treatment [19].

iv. Integrated Reflection Coefficient (IRC) Calculation

The signal region for measuring callus IRC was 0.5 mm up and downstream of the largest value in each RF signal (i.e. around two wavelengths of the reflected signal), with the largest value within the first-half of ROI (i.e. 3.0 mm depth). Signals in this region were gated by the same size of the hamming window. After the zero-padding to 512 points, the Fast Fourier transform (FFT) was conducted on the signals to give the power spectra. The power spectrum of each independent line was divided by the reference spectrum. The system-corrected spectra of the independent lines then logarithmically transformed to obtain the reflection spectra R(f). IRC (dB) was defined as:

$$IRC = \frac{1}{f_{max} - f_{min}} \int_{f_{min}}^{f_{max}} R(f) df \qquad (2)$$

where $f_{min} = 4$ MHz and $f_{max} = 8$ MHz. In the end, IRC values of independent lines were averaged.

v. Integrated Attenuation (IA) Calculation

All RF signals in the ROI were used to calculate IA. However, SoS_{cal} influenced the effective depth of ROI for calculating IA. A ratio (R_s) between SoS_0 (i.e. 1.54 mm/μs) and SoS_{cal} was used to adjust this effective depth (i.e. 6.0 mm*R_s). Such adjustment assumed that SoS_{cal} was homogenous in the bone callus.

A hamming window with an adjusted effective depth (i.e. 1.8 mm*R_s) was used to gate the signals from the point of entry to the point of exit of the ROI with a 50% overlapping between two consecutive windows [20, 21]. According to the window selection principle, six short signals in different depths were obtained from each independent line. FFT was performed to obtain the power spectra and were further divided by the power spectra of the reference signals at the corresponding depths, which were gated by the same size of the hamming window. After the system correction, spectra from independent lines with the same depth were averaged. The six averaged power spectra were then logarithmically transformed and regressed by the propagation distance. IA (dB/mm) was defined as:

$$IA = \frac{1}{f_{max} - f_{min}} \int_{f_{min}}^{f_{max}} \alpha(f) df \qquad (4)$$

where f_{min} and f_{max} were 4 and 8 MHz, respectively and α (f) (dB/mm) is attenuation coefficient from 4-8 MHz.

vi. Integrated Backscattering (IBS_corr) Calculation

After calculating IRC, the rest of the RF signals in the ROI, which was a sub-region of a 5 mm depth, were used for evaluating the callus IBS_{corr}. Since the effective depth of the sub-region was affected by SoS_{cal}, R_s was used to adjust the effective depth (i.e. 5.0 mm*R_s). RF signals in this sub-region was gated using a same size hamming window and zero-padded to 512 points. After FFT of the signals, the power spectrum of each independent line was divided by the reference spectrum, which was gated by the same size of the hamming window. The system-corrected spectrum was then logarithmically transformed to obtain the backscatter spectrum B(f). Uncorrected IBS (IBS_{uncorr}, dB) was defined as:

$$IBS_{uncorr} = \frac{1}{f_{max} - f_{min}} \int_{f_{min}}^{f_{max}} B(f) df \qquad (5)$$

where f_{min} and f_{max} were 4 and 8 MHz, respectively. To eliminate the effect from the acoustic reflection of the callus, corrected IBS (IBS_{corr}, dB) was calculated as:

$$IBS_{corr} = \frac{IBS_{uncorr}}{1 - R_{cal}^2} \qquad (6)$$

IBS_{corr} values of independent lines were ultimately averaged.

2. μCT Study

Dissected bone callus specimens were thawed at room temperature before μCT (vivaCT40, Scanco Medical, Switzerland) scanning. The density calibration of the μCT machine was obtained weekly by scanning a hydroxyapatite (HA) phantom provided by the system manufacturer.

A set of 640 contiguous axial tomographic images including the callus and tibial cortices were taken at an isotropic resolution of 21 μm. The scanning profile was set as 70kVp and 114mA with an integration time of 34 minutes. 2D tomograms, containing the bone callus, were divided equally into three

portions at its distal, middle and proximal regions, which were then compared with the respective regions segmented in US measurement.

Images were semi-automatically contoured to define the outer boundary of bone callus. A Gaussian filter with a support in 1.0 and sigma in 1.2 was applied to reduce image noise [22]. According to previous literature, a fixed global threshold in 200 was used to differentiate the mineralized and non-mineralized tissues in the consolidated bone callus [23, 24]. The binarized images were volume rendered as a 3D image and morphological data of bone callus were evaluated by a default iteration program (Scanco Medical, Switzerland). The bone tissue density (Mat.Den), trabecular number (Tb.N), thickness (Tb.Th) and separation (Tb.Sp) of the consolidated callus were evaluated (See Appendix 1 for the explanation of μCT parameters).

D. Data Analyses

The longitudinal ultrasonographic images were interpreted regionally and temporally.

The reliability of acoustic parameters was measured by intra-class correlation (ICC) coefficients with 3 US L-scan trials at each measurement time point. These parameters were also reported as Mean±SEM and presented graphically.

The Shapiro-Wilk normality test was performed on all data before using a parametric test. The trend analysis of the one-way repeated measure analysis of variance (ANOVA) was conducted on the regional acoustic parameters in two phases of DO treatment, from day 13 to day 26 (i.e. in the distraction and early consolidation phases) and from day 26 to day 47 (i.e. in the late consolidation phase).

μCT data were also reported as Mean±SEM. The stepwise multiple regression analysis was performed on μCT data of the consolidated bone callus with the acoustic parameters of the growing callus evaluated during DO treatment.

All statistical tests were conducted by SPSS 17.0 (SPSS Inc., USA) and the significant level of all tests was set at p-value = 0.05.

III. RESULTS

A. Ultrasound Study-Qualitative Evaluation

In US L-scan images (Fig. 3), the anterior distal and proximal tibial cortices were recognizable as a "double hyper-reflecting layer", a characteristic for confirming the size of the distraction gap.

Comparisons were made among the US images and the echogenicity of bone callus was increased regionally and temporally. On day 10, echgenic specks were randomly distributed in the distraction gap. With a further tibial lengthening, echogenic streaks were observed on the anterior superficial surface of bone callus, which had an increase in their echogenicity. On day 16 and day 19, those streaks became echogenically broader in the distal and proximal regions.

Nevertheless, echogenic streaks were still not bridged together on day 19.

On day 26, however, the discontinuity of bone callus disappeared and a hyper-echogenic line started to develop at the anterior part of the distraction gap. On day 33, the reverberation of bone callus occurred at the posterior part of the callus due to its multiple ultrasound reflections. On day 47, a flat hyper-echogenic surface with a broadened reverberatio line was observed at the distraction gap.

Meanwhile, tibial cortical ends could still be identified on day 33 but the accuracy of the gap measurement was largely reduced on day 40 and day 47.
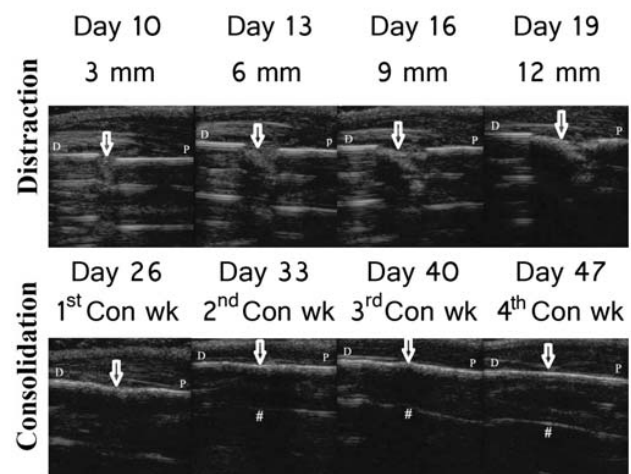

Fig. 3 Systemic comparison of representative longitudinal ultrasonographic images during DO treatment; 'D' and 'P' indicates the distal and proximal tibia, respectively. White arrow indicates the location of the bone callus. # indicates the location of the callus reverberation. '3 mm' means the tibia is distracted with a 3 mm gap distance and so on. '1st Con wk' means the first week of consolidation and so on.

B. Ultrasound Study-Quantitative Evaluation

(In this section, data are presented in the following regional priority, e.g. (a) day 13 (6 mm), data in distal, middle and proximal callus regions)

A small distraction gap in the early distraction period caused a serious signal basis in US measurement; hence, all signals collected on day 10 were only used for the graphical presentation of bone callus. Except day 10, the callus was equally divided into three regions based on its respective distracted length at the measurement time point and used for regional and temporal comparison.

i. Reliability of Acoustic Parameters

Most ICC values of the acoustic parameters were higher than 0.8 during distraction except SoS_{cal} and IRC of the middle region on day 13 (ICC = 0.53-0.68).

During the consolidation period, most ICC values of acoustic parameters were higher than 0.7. However, ICC values of IA measured in the middle region were relatively lower on day 33 and day 40 (ICC = 0.43-0.54) (Table I).

TABLE I
ICC OF ALL ACOUSTIC PARAMETERS MEASURED   DURING
DO TREATMENT

a)

ICC	Distraction Period				Consolidation Period		
SoS_{cal}	Day 13	Day 16	Day 19	Day 26	Day 33	Day 40	Day 47
Distal	0.993	0.974	0.905	0.916	0.896	0.691	0.76
Middle	0.684	0.879	0.931	0.931	0.928	0.844	0.752
Proximal	0.976	0.951	0.91	0.816	0.813	0.866	0.839

b)

ICC	Distraction Period				Consolidation Period		
IRC	Day 13	Day 16	Day 19	Day 26	Day 33	Day 40	Day 47
Distal	0.968	0.93	0.952	0.941	0.964	0.858	0.974
Middle	**0.536**	0.837	0.929	0.732	0.874	0.917	0.92
Proximal	0.899	0.935	0.973	0.829	0.76	0.847	0.858

c)

ICC	Distraction Period				Consolidation Period		
IA	Day 13	Day 16	Day 19	Day 26	Day 33	Day 40	Day 47
Distal	0.967	0.98	0.961	0.853	0.822	0.751	0.889
Middle	0.855	0.847	0.84	0.857	**0.541**	*0.43*	0.784
Proximal	0.808	0.92	0.928	0.911	**0.5**	0.65	0.958

d)

ICC	Distraction Period				Consolidation Period		
IBS_{corr}	Day 13	Day 16	Day 19	Day 26	Day 33	Day 40	Day 47
Distal	0.988	0.946	0.934	0.881	0.796	0.805	0.972
Middle	0.992	0.941	0.984	0.815	0.902	0.935	0.951
Proximal	0.976	0.975	0.982	0.983	0.931	0.977	0.892

ICC values were calculated from 3 trials and n = 7.

ii.   Speed of Sound of Callus (SoS_{cal})

The means of SoS_{cal} in three callus regions during distraction were: (a) day 13 (6 mm), 1.65±0.09, 1.61±0.03 and 1.67±0.08 mm/µs; (b) day 16 (9 mm), 1.68±0.11, 1.58±0.04 and 1.66±0.06 mm/µs; (c) day 19 (12 mm), 1.83±0.17, 1.69±0.10 and 1.79±0.13 mm/µs.

After the distraction period, the means of SoS_{cal} were: (a) day 26 (1st Con wk), 2.22±0.17, 2.15±0.16 and 2.24±0.13 mm/µs; (b) day 33 (2nd Con wk), 2.54±0.20, 2.53±0.23 and 2.77±0.21 mm/µs; (c) day 40 (3rd Con wk), 2.81±0.20, 2.54±0.16 and 2.50±0.22 mm/µs; (d) day 47 (4th Con wk), 2.41±0.22, 2.46±0.19 and 2.52±0.22 mm/µs.

Compared with the means of SoS_{cal} in the three regions on day 13, there were 34.5, 33.5 and 34.1% increases on day 26, and 46.1, 52.8 and 50.9% increases on day 47 (Fig. 4).

iii.   Integrated Reflection Coefficient (IRC)

The means of the IRC distraction were: (a) day 13 (6 mm), -38.80±2.55, -37.32±1.16 and -36.38±1.49 dB; (b) day 16 (9 mm), -38.44±2.94, -39.82±1.82 and -35.59±1.55 dB; (c) day 19 (12 mm), -36.39±3.52, -38.86±3.33 and -34.89±2.91 dB.

In the consolidation period, the means of IRC were: (a) day 26 (1st Con wk), -27.44±1.81, -28.08±1.75 and -26.41±1.30 dB; (b) day 33 (2nd Con wk), -24.80±2.35, -24.25±1.74 and -21.74±1.65 dB; (c) day 40 (3rd Con wk), -23.22±1.92, -23.98±0.97 and -25.30±2.06 dB; (d) day 47 (4th Con wk), -25.96±2.07, -25.21±1.87 and -24.58±2.13 dB.

Compared with the means of IRC in the three regions on day 13, there were 29.3, 24.8 and 27.4% increases on day 26, and 33.1, 32.4 and 32.4% increases on day 47 (Fig. 5).
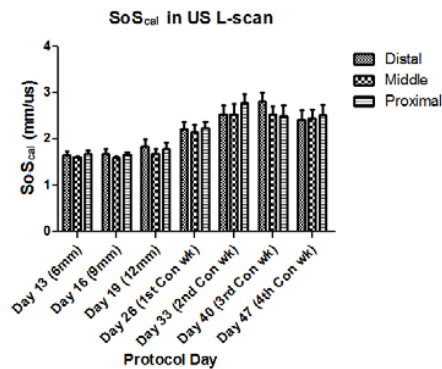

Fig. 4 Regional comparison of SoS_{cal} during DO; results were reported as Means±SEM, n = 7
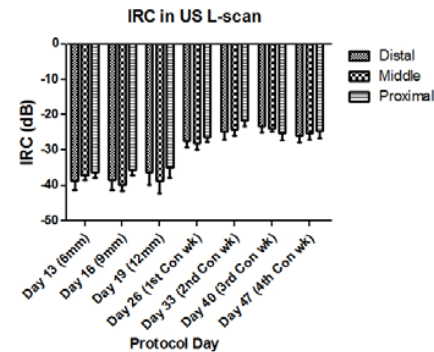

Fig. 5 Regional comparison of IRC during DO; results were reported as means±SEM, n = 7

iv. Integrated Attenuation (IA)

The means of IA during distraction were: (a) day 13 (6 mm), 3.32±0.95, 3.72±0.76 and 4.27±0.81 dB/mm; (b) day 16 (9 mm), 4.06±1.65, 3.06±0.68 and 5.80±0.86 dB/mm; (c) day 19 (12 mm), 5.70±1.54, 3.37±0.62 and 7.02±1.40 dB/mm.

The means of IA in the three regions during the consolidation period were: (a) day 26 (1st Con wk), 10.08±1.61, 8.37±1.35 and 12.23±1.40 dB/mm; (b) day 33 (2nd Con wk), 13.78±1.51, 12.50±1.43 and 15.06±1.17 dB/mm; (c) day 40 (3rd Con wk), 16.05±0.37, 12.67±0.59 and 12.85±0.80 dB/mm; (d) day 47 (4th Con wk), 13.80±1.54, 14.49±1.54 and 13.91±1.37 dB/mm.

Compared with the means of regional IA on day 13, there were 225.3, 125.0 and 186.4 % increases on day 26, and 315.7, 289.5 and 225.8% increases on day 47 (Fig. 6).

v.   Integrated Backscattering (IBS_{corr})

The means of IBS_{corr} in the three callus regions during distraction were: (a) day 13 (6 mm), -45.82±2.45, -46.63±2.72

and -47.07 ± 2.54 dB; (b) day 16 (9 mm), -47.43 ± 1.28, -45.30 ± 1.92 and -50.42 ± 2.52 dB; (c) day 19 (12 mm), -48.86 ± 2.33, -46.70 ± 3.30 and -52.12 ± 3.09 dB.

In the consolidation period, the means of IBS_{corr} were: (a) day 26 (1st Con wk), -52.57 ± 1.04, -52.43 ± 1.26 and -52.68 ± 2.29 dB; (b) day 33 (2nd Con wk), -53.07 ± 1.04, -52.43 ± 1.26 and -54.07 ± 1.10 dB; (c) day 40 (3rd Con wk), -53.07 ± 0.93, -53.91 ± 0.90 and -53.81 ± 1.54 dB; (d) day 47 (4th Con wk), -53.96 ± 2.11, -54.35 ± 1.94 and -53.94 ± 1.74 dB.

Compared with the means of regional IBS_{corr} on day 13, there were 5.5, 0.6 and 11.9% decreases on day 26, and 17.8, 16.6 and 14.6% decreases on day 47 (Fig. 7).
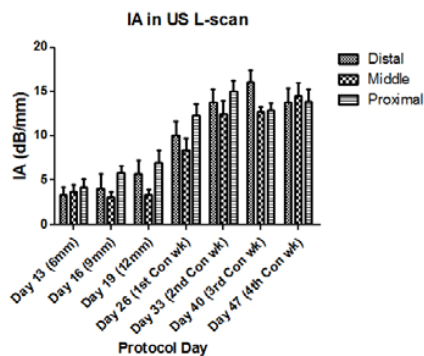

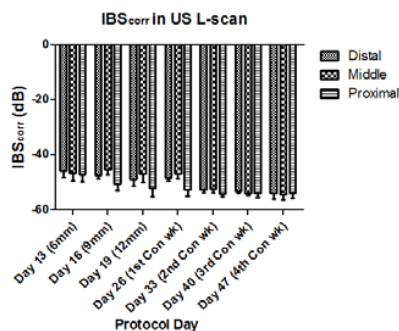Fig. 6 Regional comparison of IA during DO; results were reported as Means±SEM, n = 7

Fig. 7 Regional comparison of IBS_{corr} during DO; results were reported as Means±SEM, n = 7

vi. Trend Analysis in US Study

All parameters were tested and normally distributed (p > 0.05). SoS_{cal}, IRC and IA in the distal, middle and proximal regions of the bone callus showed a significant trend increase between day 13 and day 26 (p < 0.005). However, IBS_{corr} showed no significant trend in this period (p > 0.05).

In the late DO phase, significant trend patterns of SoS_{cal}, IRC and IA were not observed in all three regions (p > 0.05). Except the proximal region, IBS_{corr} in the distal and middle regions had significant trend decreases in the late consolidation period (p < 0.05). Meanwhile, IA in the middle region still increased significantly in the consolidation period (p = 0.047) (Table 2).

TABLE II
TREND ANALYSIS OF RADIOGRAPHIC AND ACOUSTIC
PARAMETERS DURING DO TREATMENT

p-value		^Early DO phase			^^Late DO Phase		
		Distal	Mid	Proximal	Distal	Mid	Proximal
US L-scan	SoS_{cal}	0.013*	0.015*	0.011*	0.296	0.219	0.505
	IRC	0.009**	0.002**	0.004**	0.476	0.234	0.818
	IA	0.002**	0.005**	0.001**	0.054	0.047*	0.581
	IBS_{corr}	0.273	0.86	0.125	0.020*	0.008**	0.731

Linear trend analysis of One-way Repeated Measure ANOVA was performed, p <0.05 *, <0.01**, <0.001***; ^Early DO phase referring days from day 13 to day 26 (6 mm - 1st Con wk); ^^Late DO phase referring days from day 26 to day 47 (1st Con wk- 4th Con wk).

C. µCT Study

i. Morphological Properties of Consolidated Callus

Table 3 shows the micro-structural parameters of the callus on day 47. By one-way ANOVA, there were no significant differences among the regional µCT data (p > 0.05).

TABLE III
µCT DATA OF CONSOLDIATED CALLUS ON DAY 47

Region		Mat. Den.	Tb.N	Tb.Th	Tb.Sp
Distal	Mean	682.17	3.35	0.23	0.52
	SEM	15.30	0.60	0.01	0.15
Middle	Mean	664.48	3.72	0.23	0.42
	SEM	11.91	0.56	0.01	0.11
Proximal	Mean	711.31	2.63	0.25	0.70
	SEM	18.07	0.49	0.01	0.16

Results were reported as Means±SEM, n = 7. One-way ANOVA was performed but there was no significant difference among data.

ii. Regression Between µCT of Consolidated Callus And Acoustic Parameters of Growing Callus During DO Treatment

Values of multiple correlation coefficients (R) lower than 0.6 were considered relatively weak correlations [25] (not shown in Table 4).

SoS_{cal} measured on day 16 during distraction period had already shown moderate to strong correlations with Tb.Th and Mat.Den of consolidated bone callus (R > 0.6, p < 0.01). On day 19, IA even showed higher correlations with Tb.Th and Mat.Den (R > 0.7, p < 0.001), and this contributed to about 50% variance in both structural properties of consolidated callus.

The correlations of SoS_{cal} and IA with µCT data were reduced during consolidation, which were lower than 0.6 (not shown in Table 4). Instead, IBS_{corr} measured in the late DO phase became more significantly correlated to the structural properties of consolidated callus, which were Tb.Th, Tb.Sp and Mat.Den on day 40 (R > 0.68, p < 0.01). IBS_{corr} also contributed to 47-51% variance in these structural properties of consolidated callus (Table IV).

TABLE IV
PREDICTION OF CONSOLIDATED CALLUS PROPERTIES AT THE END
OF STUDY (Day 47) BY ACOUSTIC PARAMETER AT DIFFERENT
MEAUREMENT TIME POINTS

μCT parameter	Protocol Day	Predictor	R	R^2
Tb.N	Day 26 (1st Con wk)	IA	0.626**	0.392
Tb.Th	*Day 16 (9 mm)*	*SoS$_{cal}$*	*0.656** *	*0.430*
	Day 19 (12 mm)	*IA*	*0.702*** *	*0.493*
	Day 40 (3rd Con wk)	IBS$_{corr}$	0.711***	0.506
Tb.Sp	Day 40 (3rd Con wk)	IBS$_{corr}$	0.717***	0.514
Mat.Den	*Day 16 (9 mm)*	*SoS$_{cal}$*	*0.632** *	*0.399*
	Day 19 (12 mm)	*IA*	*0.71*** *	*0.504*
	Day 26 (1st Con wk)	IBS$_{corr}$	0.683**	0.466
	Day 40 (3rd Con wk)	IBS$_{corr}$	0.687**	0.472

Regression was performed with the regional μCT on day 47 and acoustic data at different measurement time points. Regional acoustic data on the same measurement time point were pooled together in the calculation of the regression. Only the correlations with R> 0.6 and p <0.05 were reported; p <0.05 *, <0.01**, <0.001***

IV. DISCUSSION AND CONCLUSION

Previous histological studies have found that bone callus grows in a characterized regional pattern during the early DO phase [14, 16, 17]. If this growth pattern can be detected *in-vivo* as early as possible during DO treatment, it may serve as a biomarker for recognizing unfavourable treatment conditions such as delayed union or premature consolidation [16]. In light of this, the present study evaluated the effectiveness of ultrasound imaging in monitoring normal bone callus growth in a rabbit tibial DO model.

In the early distraction phase, a distinct amount of regional mineralization of bone callus was revealed by echogenic signals in the longitudinal US images. On day 16 and day 19, the appearance of a well-defined superficial surface was observed in the distal and proximal regions but not in the middle region (Fig. 3). This indicated that the bone callus was growing from the proximal and distal host bone surfaces (HSBs) towards the centre of the distraction gap. Such ultrasonographic observation could be explained by the mechano-biology during distraction. Under the external tensile loading, there was a high strain-rate in the middle region of bone callus. This high mechanical strain stimulated fibroblasts to continuously produce collagen fibers and suppressed differentiation between osteoprogenitor cells and active osteoblasts, which further restrained bone mineralization in the middle region [26]. However, the strain level on the proximal and distal sides of the distraction gap was much lower, creating a more favourable condition for osteoblasts to ossify the callus at the distal and proximal regions [27, 28]. Because of these cellular responses, the ultrasonographic characteristic pattern found in the present study reflected a higher mineralization at the proximal and distal regions of the callus than that in the middle region. This undulating mineralization pattern was concurred with the previous histological and CT studies during distraction, which classified the bone callus into several zones based on their tissue

structures and degrees of bone mineralization, respectively [16, 17].

In the consolidation phase, the rapid increase in bone callus surface density and the callus bridging caused a strong reflection of the ultrasound wave (Fig. 3), thus greatly restricting the ultrasonographic demonstration of bone callus condition. Nevertheless, the appearance of callus reverberation observed in B-mode images supports that the callus density increases during consolidation.

Conventional semi-quantitative scoring on the bone callus condition in B-mode images is a subjective interpretation based on the clinician's experience [29]. In the present study, however, the acoustic parameters are directly measured from the RF signals reflected by bone callus, which allows for a more objective evaluation. Previous study reported that the low bone density of the early callus growth could not be detected by conventional plain radiography unless there was a 40% change in its radiodensity during the consecutive radiographic measurement [14]. But SoS$_{cal}$, IRC and IA measured in the three callus regions showed significant trend increases over time during early DO phase of this study. The increase of IRC reflects an increase of the callus surface density while the increase of SoS$_{cal}$ and IA indicates the growth of callus density and its internal structure (e.g. trabecular bone). Besides, during the consolidation phase, there were significant trend decreases in IBS$_{corr}$ of the distal and middle callus regions in the late DO phase. Because of significant increase of callus material density and the callus bridging, strong ultrasound reflection caused a large reduction of ultrasound backscattering from the internal bone structure, which resulted in the decrease of IBS$_{corr}$ during consolidation. These findings indicate that the acoustic parameters are more sensitive than radiographic density to bone callus changes. This can help with examining the effectiveness of pharmacological [10] and non-pharmacological promotion [24] of bone regeneration during DO treatment.

The healing bone strength is determined by its material density and microstructure [30] and is an important outcome parameter of the DO treatment. In this study, there were moderate to strong correlations of SoS$_{cal}$ and IA measured during distraction with the micro-architectural properties of consolidated bone callus (R = 0.6-0.7). SoS$_{cal}$ and IA measured during this phase contributed to about 40-50% variance of the structural properties of consolidated callus. However, during the late consolidation phase, the predictive power of SoS$_{cal}$ and IA on the structural properties of consolidated bone callus was largely reduced. Instead, IBS$_{corr}$ measured at the late DO phase became more correlated with the consolidated callus structural properties (R = 0.6-0.7) and IBS$_{corr}$ accounted for 47-51% of such variance. Such prediction offered by the acoustic parameters may aid in the evaluation of the prognosis of the treatment.

To conclude, the present study successfully demonstrates that our US method can provide a repeatable qualitative and quantitative assessment on normal bone callus growth during DO treatment, especially in the early phase. Because of its non-ionizing property and predictive power for end point callus density and structural properties, this US method should be

further validated for clinically monitoring the bone regeneration of DO patients.

APPENDIX

Appendix I shows the explanation of μCT parameters used in this paper.

APPENDIX I
EXPLANATION OF μCT MICRO-ARCHITECTURE PARAMETERS

Abbreviation	Variable	Description	Standard unit
Mat.Den	Callus mineral density	Mineral density of the segmented callus volume	mg/cc of HA
Tb.N	Trabecular number	Measure of the average number of trabeculae per unit length (by direct 3D method)	mm⁻¹
Tb.Th	Trabecular thickness	Mean thickness of trabeculae (by direct 3D method)	mm
Tb.Sp	Trabecular separation	Mean distance between trabeculae (by direct 3D method)	mm

REFERENCES

[1] J. Aronson, H. D. Shin, "Imaging techniques for bone regenerate analysis during distraction osteogenesis", Journal of Pediatric Orthopaedics, vol 23, pp.550-560, 2003.
[2] R. Lisa, A. V. Everts, A. L. J. J. Broncker, "Bone regeneration during distraction osteogenesis", Odontology, vol 97, pp.63-75, 2009.
[3] T. Hughes, G. V. Maffulli N, Fixsen JA., "Imaging in bone lengthening. A review", Clinical Orthopaedics and Related Research, pp.50-53, 1994.
[4] BEIR, Health risks from exposure to low levels of ionizing radiation : BEIR VII, Phase 2. . Washington, D.C. : National Academies Press, 2006.
[5] D. Richter, M. P. Hahn, P. A. W. Ostermann, A. Ekkernkamp, G. Muhr, "Ultrasound monitoring of callus distraction: An alternative to radiological diagnosis?", Langenbecks Archiv Fur Chirurgie, pp.931-933, 1996.
[6] N. Maffulli, T. Hughes, J. A. Fixsen, "Ultrasonography monitoring of limb lengthening", Journal of Bone and Joint Surgery-British Volume, vol 74, pp.130-132, 1992.
[7] C. Bruno, S. Minniti, E. Buttura-Da-Prato, M. Albanese, P. F. Nocini, R. Pozzi-Mucelli, "Gray-scale ultrasonography in the evaluation of bone callus in distraction osteogenesis of the mandible: initial findings", European Radiology, vol 18, pp.1012-1017, 2008.
[8] N. Adolphs, C. Kunz, P. Pyk, B. Hammer, B. Rahn, "Callus mineralization following distraction osteogenesis of the mandible monitored by scanning acoustic microscopy (SAM)", Journal of Cranio-Maxillofacial Surgery, vol 33, pp.314-317, 2005.
[9] N. Adolphs, C. Kunz, P. Pyk, B. Hammer, B. Rahn, "Callus mineralization following distraction osteogenesis of the mandible monitored by scanning acoustic microscopy (SAM)", Journal of Cranio-Maxillofacial Surgery, vol 33, pp.314-317, 2005.
[10] C. W. Chan, L. Qin, K. M. Lee, M. Zhang, J. C. Y. Cheng, K. S. Leung, "Low intensity pulsed ultrasound accelerated bone remodeling during consolidation stage of distraction osteogenesis", Journal of Orthopaedic Research, vol 24, pp.263-270, 2006.
[11] J. E. Tis, R. H. Meffert, N. Inoue, E. F. McCarthy, M. S. Machen, K. A. McHale, E. Y. S. Chao, "The effect of low intensity pulsed ultrasound applied to rabbit tibiae during the consolidation phase of distraction osteogenesis", Journal of Orthopaedic Research, vol 20, pp.793-800, 2002.
[12] R. Aleksyniene, Eckardt, H., Bundgaard, K., Lind, M, and Hvid, I., "Effects of parathyroid hormone on newly regenerated bone during

distraction osteogenesis in a rabbit tibial lengthening model. A pilot study.", Medicina (Kaunas), pp.38-48, 2006.
[13] K. B. Jones, N. Inoue, J. E. Tis, E. F. McCarthy, K. A. McHale, E. Y. S. Chao, Quantification of the microstructural anisotropy of distraction osteogenesis in the rabbit tibia. 2005.
[14] J. Aronson, "Basic science and biological principles of distraction osteogenesis", in Limb Lengthening and reconstructive surgery, S. Robert Rozbruch SI, editor. Ed. New York: Informa Healthcare, 2007, pp.19-42.
[15] J. Aronson, "Experimental and clinical experience with distraction osteogenesis", Cleft Palate-Craniofacial Journal, vol 31, pp.473-481, 1994.
[16] J. Aronson, B. Good, C. Stewart, B. Harrison, J. Harp, "Preliminary studies of mineralization during distraction osteogenesis", Clinical Orthopaedics and Related Research, pp.43-49, 1990.
[17] G. Li, A. H. R. W. Simpson, J. Kenwright, J. T. Triffitt, "Assessment of cell proliferation in regenerating bone during distraction osteogenesis at different distraction rates", Journal of Orthopaedic Research, vol 15, pp.765-772, 1997.
[18] R. N. McCarthy, L. B. Jeffcott, R. N. McCartney, "Ultrasound speed in equine cortical bone: Effects of orientation, density, porosity and temperature", Journal of Biomechanics, vol 23, pp.1139-1143, 1990.
[19] A. A. Hijazy, S. M. Smoudi H, Qaddoum N, Al Nashash H, Ramesh K G, "Quantitative monitoring of bone healing process using ultrasound", Journal of the Franklin Institute, vol 343, pp.495-500, 2006.
[20] Y. P. Huang, Y. P. Zheng, S. F. Leung, A. F. T. Mak, "Reliability of measurement of skin ultrasonic properties in vivo: a potential technique for assessing irradiated skin", Skin Research and Technology, vol 13, pp.55-61, 2007.
[21] Y. P. Huang, Y. P. Zheng, S. F. Leung, A. P. C. Choi, "High frequency ultrasound assessment of skin fibrosis: Clinical results", Ultrasound in Medicine and Biology, vol 33, pp.1191-1198, 2007.
[22] O. Gauthier, R. M□ler, D. von Stechow, B. Lamy, P. Weiss, J.-M. Bouler, E. Aguado, G. Daculsi, "In vivo bone regeneration with injectable calcium phosphate biomaterial: A three-dimensional micro-computed tomographic, biomechanical and SEM study", Biomaterials, vol 26, pp.5444-5453, 2005.
[23] F. M. Elise, D. M. Zachary, B. C. Karen, J. P. Anthony, L. B. George, A. E. Thomas, C. G. Louis, "Micro-computed tomography assessment of fracture healing: Relationships among callus structure, composition, and mechanical function", Bone, vol 44, pp.335-344, 2009.
[24] R. Aleksyniene, J. S. Thomsen, H. Eckardt, K. G. Bundgaard, M. Lind, I. Hvid, "Three-dimensional microstructural properties of regenerated mineralizing tissue after PTH (1-34) treatment in a rabbit tibial lengthening model", Journal of Musculoskeletal & Neuronal Interactions, vol 9, pp.268-277, 2009.
[25] J. Cohen, Statistical power analysis for the behavioral sciences 2nd. NJ: Hillsdale, 1988.
[26] D. R. Carter, G. S. Beaupr, N. J. Giori, J. A. Helms, "Mechanobiology of skeletal regeneration", Clinical Orthopaedics and Related Research, vol 355, pp.S41-S55, 1998.
[27] M. Mullender, A. J. El Haj, Y. Yang, M. A. van Duin, E. H. Burger, J. Klein-Nulend, "Mechanotransduction of bone cells in vitro: mechanobiology of bone tissue", Medical & Biological Engineering & Computing, vol 42, pp.14-21, 2004.
[28] H. Isaksson, O. Comas, C. C. van Donkelaar, J. Mediavilla, W. Wilson, R. Huiskes, K. Ito, "Bone regeneration during distraction osteogenesis: Mechano-regulation by shear strain and fluid velocity", Journal of Biomechanics, vol 40, pp.2002-2011, 2007.
[29] L. B. Kaban, P. Thurmuller, M. J. Troulis, J. Glowacki, D. Wahl, B. Linke, B. Rahn, D. H. Perrott, "Correlation of biomechanical stiffness with plain radiographic and ultrasound data in an experimental mandibular distraction wound", International Journal of Oral and Maxillofacial Surgery, vol 32, pp.296-304, 2003.
[30] E. Seeman, "Bone quality: the material and structural basis of bone strength", Journal of Bone and Mineral Metabolism, vol 26, pp.1-8, 2008.